Neuron, Vol. 39, 133–146, July 3, 2003, Copyright ©2003 by Cell Press

Contribution of *Drosophila* DEG/ENaC Genes to Salt Taste

Lei Liu,[1] A. Soren Leonard,[1] David G. Motto,[1,3] Margaret A. Feller,[1] Margaret P. Price,[1] Wayne A. Johnson,[2] and Michael J. Welsh[1,2,*]

[1]Howard Hughes Medical Institute and Department of Internal Medicine

[2]Department of Physiology and Biophysics

Roy J. and Lucille A. Carver College of Medicine

University of Iowa

Iowa City, Iowa 52242

Summary

The ability to detect salt is critical for the survival of terrestrial animals. Based on amiloride-dependent inhibition, the receptors that detect salt have been postulated to be DEG/ENaC channels. We found the *Drosophila* DEG/ENaC genes *Pickpocket11* (*ppk11*) and *Pickpocket19* (*ppk19*) expressed in the larval taste-sensing terminal organ and in adults on the taste bristles of the labelum, the legs, and the wing margins. When we disrupted PPK11 or PPK19 function, larvae lost their ability to discriminate low concentrations of Na^+ or K^+ from water, and the electrophysiologic responses to low salt concentrations were attenuated. In both larvae and adults, disrupting PPK11 or PPK19 affected the behavioral response to high salt concentrations. In contrast, the response of larvae to sucrose, pH 3, and several odors remained intact. These results indicate that the DEG/ENaC channels PPK11 and PPK19 play a key role in detecting Na^+ and K^+ salts.

Introduction

Survival of most terrestrial animals requires the ability to detect environmental salt, a nutrient essential for fluid and electrolyte homeostasis (Contreras and Lundy, 2000; Denton, 1982; Lindemann, 1996). The gustatory system is the main chemical sensory modality that recognizes NaCl and other salts. This sensory system allows animals to detect and ingest salt, to discriminate between different salts, and to avoid high salt concentrations. Although recent work has identified receptors that detect sweet and bitter substances, our understanding of the receptors that detect salt is limited (Halpern, 1998; Herness and Gilbertson, 1999; Kinnamon and Margolskee, 1996; Lindemann, 1996).

Amiloride-sensitive degenerin/epithelial Na^+ channels (DEG/ENaC) have been considered good candidates to serve as receptors for salt taste (Halpern, 1998; Herness and Gilbertson, 1999; Kinnamon and Margolskee, 1996; Lindemann, 1996). In some cases (for example, with coexpression of α, β, and γ ENaC subunits), these channels form constitutively open, cation-selective pores (Canessa et al., 1994; McDonald et al., 1995). It is hypothesized that an increased cation concentration at their surface depolarizes the cell membrane, thereby initiating action potentials and the release of neurotransmitters (Boughter and Smith, 1998; DeSimone et al., 1981; Kinnamon and Cummings, 1992).

The localization of α, β, and γ ENaC subunits in mammalian taste receptor cells and the finding that aldosterone increased their apical localization suggested that DEG/ENaC channels may be involved in salt taste (Lin et al., 1999; Kretz et al., 1999). Additional evidence suggesting that DEG/ENaC channels are involved in salt taste comes from observations that amiloride can impair the gustatory response to NaCl (Boughter and Smith, 1998; Scott and Giza, 1990). Extracellular amiloride blocks most DEG/ENaC channels (Garty and Palmer, 1997). However, studies testing the inhibitory effect of amiloride on salt taste have reported varying results in different animal species and in tests done by different laboratories. For example, amiloride does not completely inhibit vertebrate responses to NaCl, amiloride fails to inhibit salt taste in some species, and behavioral and physiological assays of salt taste from different laboratories have shown discrepant results and interpretations (Halpern, 1998; Herness and Gilbertson, 1999; Lindemann, 1996). Some of the apparent discrepancies in the literature may arise from differences in the Na^+ diet of the different species. However, some of the differences likely also relate to the use of amiloride and its analogs. The concentrations of amiloride required to inhibit DEG/ENaC channels can also vary substantially. For example, ENaC can be inhibited by 0.1–1 μM amiloride, whereas the acid-sensing ion channel-1 (ASIC1) requires 100 μM to 1 mM (Waldmann et al., 1997). Moreover, amiloride is not a specific inhibitor of DEG/ENaC channels. It can also inhibit other membrane transport processes, including Na^+/H^+ antiporters, Na^+/Ca^{2+} exchangers, the Na^+ pump, cyclic nucleotide-gated channels, and Ca^{2+} channels (Frings et al., 1992; Garty and Palmer, 1997; Luciani et al., 1992; Tang et al., 1988). As increasing concentrations of amiloride are applied to gustatory organs, the effect on other transporters becomes a greater confounding factor. Thus, using amiloride-sensitivity as the criterion for assigning a molecular mechanism could be misleading. In addition, amiloride-insensitive mechanisms, including Na^+/H^+ antiporters (Lundy et al., 1997) and cation diffusion through tight junctions (Lindemann, 1996), have been proposed to participate in mammalian NaCl salt taste.

To learn whether DEG/ENaC channels are involved in salt taste, we studied *Drosophila melanogaster* as a model system. The behavioral response of *Drosophila* to salt is in several ways similar to that in mammals. In behavioral assays, *Drosophila* larvae discriminate NaCl from water and distinguish between NaCl and KCl (Miyakawa, 1981; Miyakawa, 1982). Low concentrations ($<$200 mM) of NaCl are attractive, whereas high concentrations ($>$1 M) are repulsive. Amiloride has also been reported to reduce the behavioral preference for salt in *Drosophila* larvae (Jenkins and Tompkins, 1990). However, high amiloride concentrations (5 mM) were re-

*Correspondence: michael-welsh@uiowa.edu

[3]Present address: Department of Pediatrics, University of Michigan, Ann Arbor, Michigan.

Table 1. Cloned PPK Gene Chromosomal Location and Annotation

Gene Name	Accession Number	Chromosomal Location	Gene Annotation Number
ppk	AF043263	35A1	PPK
rpk	AF043264	82C5-D1	RPK
ppk4	AF024691, U53479, AY226538	53C11-C13	Nach
ppk6	AY226539	56F11	CG11209
ppk7	AY226540	26C4-D1	CG9499
ppk10	AY226541	31E2-E3	N/A
ppk11	AY226542	30D1	CG4110
ppk12	AY226543	58D8-E1	CG10972
ppk13	AY226544	39A6-A7	CG14398
ppk14	AY226545	26C4-D1	CG9501
ppk16	AY226546	30D1	CG4110
ppk19	AY226547	99B9-B10	CG18287
ppk20	AY226548	99B8-B9	CG7577
ppk21	AY226549	99B8-B9	CG12048
ppk23	AY552550, AY226551	16B4-B6	CG8527
ppk28	AY226552, AY226553	15A7	CG4805

quired, raising questions about the responsible mechanisms. In larvae, gustation depends on the terminal organ, which sits at the front of the larval head. The terminal organ contains 30 to 40 taste receptor cells in a structure that shows morphologic similarity to the mammalian taste bud (Python and Stocker, 2002). In adults, gustatory organs are present at many sites, including taste bristles located on the labelum of the proboscis, on the tarsal segment of the leg, on the surface of the mouth and within the pharynx, on the wing margins, and on the ovipositor (Stocker, 1994). When a fly steps on a food source, taste bristles on the legs contact the food. If an attractive signal is detected, the fly extends the proboscis to further examine the food source. If a positive signal registers, the fly opens the labelar lobes exposing taste papillae on the surface of the mouth. Appropriate stimulation of the papillae results in ingestion (Dethier, 1976; Pollack and Balakrishnan, 1997). Taste hairs on the wing may be used during passage through narrow spaces, and on the ovipositor they may be used in selecting sites for depositing eggs (Pollack and Balakrishnan, 1997; Singh, 1997).

Drosophila were also of interest as a model system because a large number of DEG/ENaC genes have been predicted from the *Drosophila* genome (Littleton and Ganetzky, 2000). In this work, we tested the hypothesis that DEG/ENaC genes contribute to salt taste.

Results

Identification of *Drosophila* PPK Genes

We searched the *Drosophila* genomic sequence database and identified ~25 candidate DEG/ENaC genes, including *Pickpocket* (*ppk*) and *Ripped Pocket* (*rpk*) (Adams et al., 1998a; Darboux et al., 1998). Using RT-PCR, we cloned 14 *ppk* genes from adult *Drosophila* mRNA. Table 1 shows their chromosomal location. Although the genes tended to be scattered throughout the genome, some of the PPK genes were found in close proximity to each other. For example, *ppk7* was ~630 bp from *ppk14*; *ppk11* was ~70 bp from *ppk16*; and *ppk19*, *ppk20*, and *ppk21* were clustered ~2.1 and 3.6 Kb from each other.

The predicted amino acid sequences of the 14 PPK proteins and PPK and RPK are shown in Figure 1. The M2 region was highly conserved (shaded gray), including the absolute conservation of a G-X-S sequence that is thought to contribute to the channel pore (Kellenberger et al., 1999). Fourteen cysteines (numbered Cl to Cl4) with relatively preserved spacing were present in the large extracellular domain. In addition, nearly all of the PPK proteins showed conservation of some sequences observed in other DEG/ENaC subunits, including an T/S-X-h-H-G (where "h" indicates a hydrophobic residue) sequence preceding M1, an F-P-h-h-T-h-C sequence following M1, and a G-X-C-X-X-F-N sequence at C4. Other conserved sequences identified by a CLUSTALW alignment are highlighted in Figure 1. As with other DEG/ENaC members, all the proteins contained numerous consensus sequences for N-linked glycosylation in the extracellular domain (blue underlined). Other than the T/S-X-h-H-G sequence, the intracellular N and C termini were minimally conserved. The N termini was predicted to vary in length from 32 residues in PPK13 to 126 residues in PPK11. Likewise, the C terminus was predicted to vary in length from an estimated 9 residues in PPK16 to 93 residues in PPK28. In the C terminus of ENaC subunits, disruption of a P-P-P-X-Y-X-X-L motif that binds W-W domain proteins causes the genetic disease Liddle's syndrome (Schild et al., 1996; Snyder et al., 1995). Interestingly, PPK28 had this same C-terminal sequence (pink). We identified splice variants in three PPK genes including PPK4, PPK23, and PPK28; the sequence (green and underlined) was missing from some transcripts.

A specific residue that lies just N-terminal to M2, the "Deg residue" (Figure 1), plays a key role in channel function. Mutation of the Deg residue constitutively activates several DEG/ENaC channels, including ASIC2 (also called BNC1 [Adams et al., 1998b; Waldmann et al., 1996]), causes cell swelling and degeneration of neurons in vivo (Chalfie and Wolinsky, 1990; Driscoll and Chalfie, 1991), and alters ion selectivity of ASIC2. These data suggest that the Deg residue plays a key role in channel open state and ion selectivity. In all previously reported wild-type DEG/ENaC proteins, the Deg residue has a relatively small side chain (Gly, Ala, or Ser), and mutation to a more bulky residue (e.g., Val or Leu)

caused constitutive channel activation. A Gly, Ala, or Ser occupies the Deg position in most of the new predicted PPK proteins (Figure 1). However interestingly, PPK7, PPK10, PPK13, PPK14, and PPK23 contain a Val which has a bulky side chain at this site.

To examine the relationship between the various PPK genes and their relationship to several other DEG/ENaC family members, we constructed a phylogenetic tree (Figure 2). The *Drosophila* members appear to be more closely related to each other than to DEG/ENaC channels from other species. Thus, *Drosophila* PPK genes may form a distinct subfamily. PPK proteins with adjacent chromosomal locations were more similar to each other than to other PPK proteins (Figure 2 and Table 1).

Expression of PPK Genes in the Salt-Sensing Terminal Organ

Salt taste in larvae has been associated with the terminal organ (Heimbeck et al., 1999; Opplinger et al., 2000). When the terminal organ was disrupted by promoter-driven toxic gene expression, the preference of larvae for low salt concentrations was abolished (Heimbeck et al., 1999). Although the larval ventral pits may also be involved in salt detection, without the terminal organ they are not sufficient to detect salt (Heimbeck et al., 1999; Smith, 2001).

To determine if PPK genes are expressed in the terminal organ, we examined their expression pattern using in situ hybridization of whole-mount embryos. We detected *ppk11* expression in three neurons of the terminal organ and *ppk19* in at least one terminal organ neuron (Figures 3A and 3C). We also found *ppk11* expressed in the ventral pits and the tracheal system (Figure 3A and Liu et al., 2003). Neither *ppk4* nor *ppk28* was expressed in the terminal organ (Figures 3D and 3E).

To further determine whether *ppk11* and *ppk19* were expressed in the terminal organ, we used the Gal4/UAS system to drive eGFP expression. As a control, we used the panneuronal promoter elav; in *elav* × *eGFP* transgenics, both the terminal organ and dorsal organ were readily visualized (Figure 3F). The *ppk11* promoter drove expression in the larval terminal organ (Figures 3G–3I). Confocal microscopy of third instar larvae revealed expression in three terminal organ neurons; Figure 3H shows three sections through the terminal organ, each showing a positive neuron. Occasionally, we also observed eGFP fluorescence extending out the dendrite toward the terminal organ pit (Figure 3I). We also found *ppk11* promoter-driven eGFP in the tracheal system but not in the ventral pits (Figure 3G and Liu et al., 2003). The lack of *ppk11* promoter expression in the ventral pits suggests that the 2 kb *ppk11* promoter may be a weak or incomplete promoter. Moreover, with the *ppk11* promoter, eGFP expression was not detected until the late first or early second instar larval stage. The *ppk19* promoter was also expressed in three neurons in the terminal organ (Figure 3J). Thus, both in situ hybridization and promoter-driven eGFP expression placed *ppk11* and *ppk19* expression in the terminal organ.

Even though we detected no transcripts by in situ hybridization, we found that the promoters for three additional PPK genes produced eGFP expression in the terminal organ. We detected activity from the *ppk6* promoter in one terminal organ neuron, *ppk10* in one terminal and one dorsal organ neuron, and *ppk13* in one terminal and four dorsal organ neurons (Figures 3K–3M). These PPK gene promoters were also differentially expressed in other regions (data not shown). Neither the *ppk4* nor the *ppk28* promoters drove eGFP expression in the terminal organ. However, consistent with the in situ hybridization, the *ppk4* promoter drove eGFP expression in the tracheal system and in ventral pits (Figure 3N). The *ppk28* promoter drove eGFP expression predominantly in the ventral pits (Figure 3O). Because neither in situ hybridization nor promoter-driven eGFP expression showed *ppk4* or *ppk28* expression in the terminal organ, we used them as negative controls in subsequent experiments.

Expression of PPK11 in Adult *Drosophila* Taste Organs

In larvae and adult *Drosophila*, the taste organs consist of bipolar taste receptor neurons surrounded by supporting cells that form a specialized structure containing a pore at its tip. In adults, taste receptors are widely distributed, including on the labelum of the proboscis and the internal mouth. The labelum has 62 taste bristles distributed on the basal, medial, and lateral surface (Shanbhag et al., 2001; Singh, 1997). Each taste bristle contains two to five neurons: one is a mechanosensory neuron, and the remainder (one to four) are chemosensory neurons. The dendrites of chemosensory neurons extend deep into the hair lumen to lie close to the open pore, whereas the dendrites of mechanosensory neurons remain at the base of the hair.

The *ppk11* promoter drove eGFP expression in some (Figures 3Q and 3R) taste bristles on the labelum of the proboscis. For comparison, Figure 3P shows expression driven by the *elav* neuronal promoter. *ppk11* was usually expressed in two to four neurons per bristle, and the dendrites extended out toward the tip of the bristle (Figure 3R). Because each taste bristle has only one mechanosensory neuron, expression of *ppk11* in more than one neuron suggests that it is expressed in at least some of the chemosensory neurons, suggesting a role in gustation. We also found the *ppk11* promoter expressed in what are probably internal taste organ neurons (yellow arrowhead, Figures 3Q and 3R) (Shanbhag et al., 2001; Singh, 1997). Thus, as in larvae, the *ppk11* expression pattern positions it where it could be involved in detecting salt concentration.

We also observed PPK gene expression at other sites of gustation in the adult. *ppk11* and *ppk19* were expressed in hairs on the tibia and femur (Figures 3S and 3T). *ppk11* (Figure 3U) and *ppk13* (Figure 3V) but not *ppk19* (Figure 3T) were expressed in hairs on the tarsi of the leg. In addition, the hairs in the wing margin showed expression of both *ppk11* and *ppk19* (Figures 3W and 3X).

Disruption of the Behavioral Response to Salt with a Dominant-Negative PPK Construct

To test the hypothesis that PPK genes function in salt taste, we generated dominant-negative constructs for PPK11 and PPK19 ($PPK11^{DN}$ and $PPK19^{DN}$) that encode the N-terminal and the first predicted transmembrane

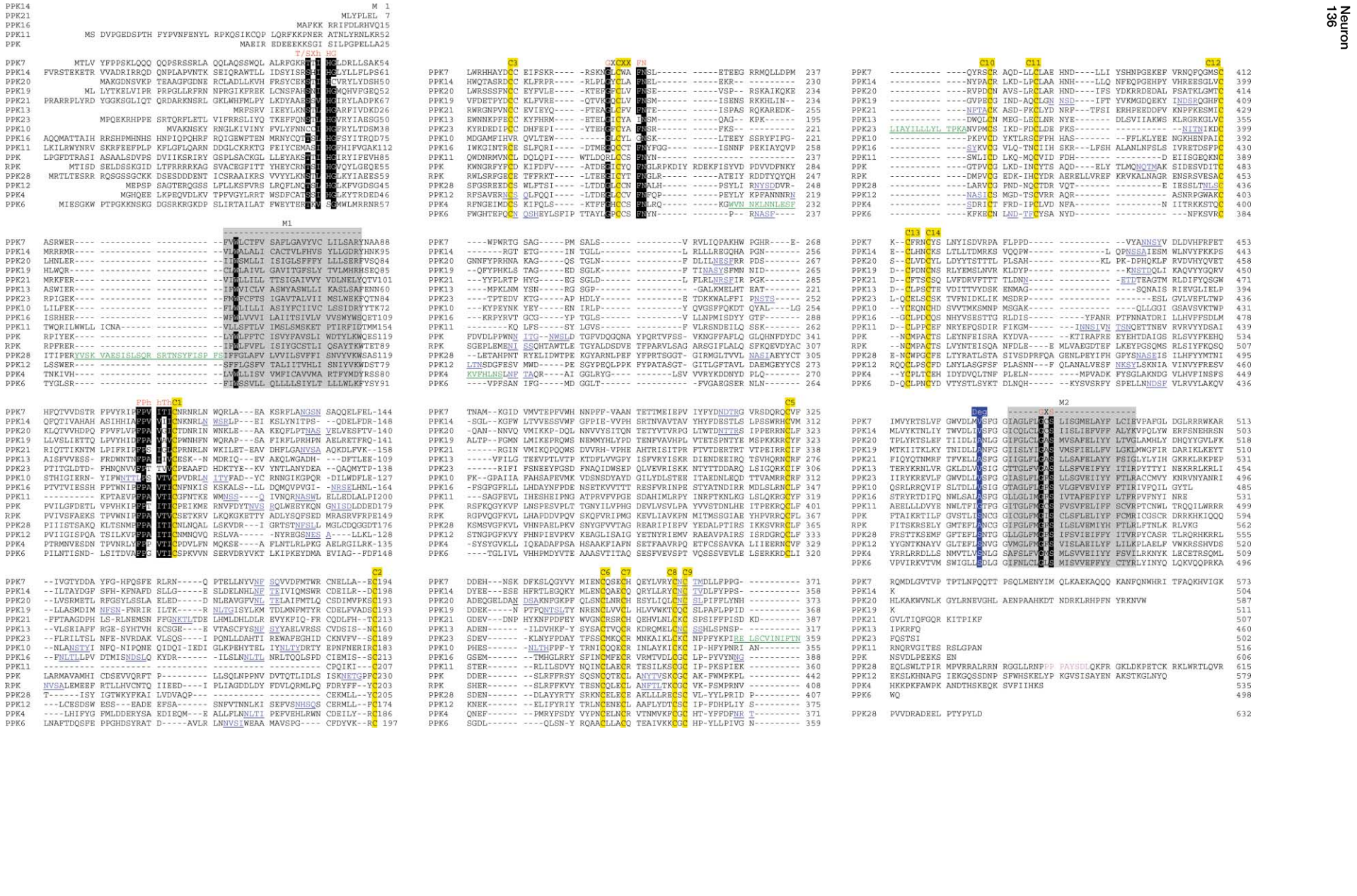

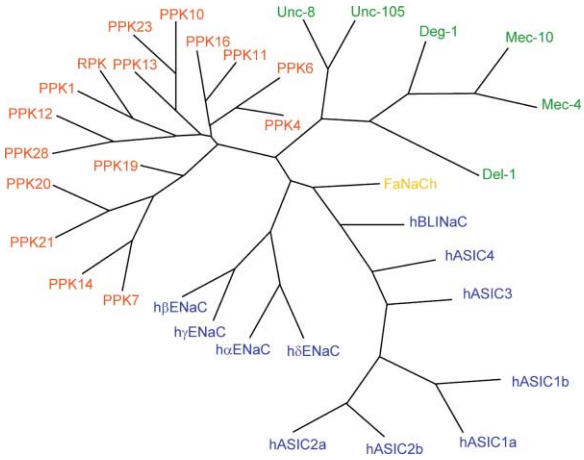

Figure 2. Phylogenetic Tree

Comparison of the 16 cloned *Drosophila* DEG/ENaC proteins with selected family members from *C. elegans*, *H. aspersa*, and mammals. See Experimental Procedures for construction of tree.

domain sequence. We produced similar constructs for PPK4 and PPK28 (PPK4^{DN} and PPK28^{DN}) to test as controls. Our strategy was based on earlier work showing that the three ENaC subunits form relatively strong interactions mediated in part through N-terminal residues (Adams et al., 1997). The N-terminal portion of γENaC associated with full-length subunits early during biosynthesis, markedly reducing the amount of wild-type protein and Na^+ current. In *C. elegans*, in vivo transgenic expression of a Mec-4 N-terminal protein mimicked the loss-of-function phenotype of Mec-4 mutants and suppressed a gain-of-function phenotype of a constitutively active Mec-4 allele (Hong et al., 2000). To test the dominant-negative effect of PPK11^{DN}, we expressed it and PPK11 (each tagged at the carboxyl termini with His6 and V5 epitopes) in the *Drosophila* S2 cell line. Figure 4 shows that PPK11^{DN} reduced the amount of PPK11 protein. The band from PPK11^{DN} was not usually well seen. Following translation, it is probably rapidly degraded, thereby accounting for its ability to reduce levels of PPK11.

To assess salt-taste behavior, third instar larvae were placed in the middle of a petri dish in which half the surface contained agar prepared with water and half contained agar prepared with 10 mM NaCl. Consistent with earlier reports (Heimbeck et al., 1999; Miyakawa, 1981; Miyakawa, 1982), wild-type larvae (genotypes *elav-Gal4*, *UAS-ppk11.24^{DN}*) preferred 10 mM NaCl to water (Figure 5A). When crossed with a panneuronal driver *elav*, two independent *ppk11^{DN}* lines failed to distinguish 10 mM NaCl and water.

Because the *elav* driver generates expression in all neurons, we could not exclude the possibility that defective salt taste in *elav* × *ppk11^{DN}* was due to an effect in the central nervous system. For example, in shaker K^+ channel mutants, defective salt-taste behavior resulted from a central rather than a peripheral nervous system defect (Balakrishnan and Rodrigues, 1991). Therefore, we drove *ppk11^{DN}* expression with the *GH86* promoter, which drives expression in the dorsal and terminal organs; it also drives expression in the epidermis, enocytes, and pharyngeal muscle (Heimbeck et al., 1999). We found defective salt taste in *GH86* × *ppk11.24^{DN}* larvae (Figure 5B). Because the *GH86* driver is located on the X chromosome, males should produce approximately twice as much Gal4 as females. Thus, in a *GH86* × *ppk11.24^{DN}* cross, the dominant-negative effect should be greater in males than females. As predicted, males showed a greater salt-taste defect than females (Figure 5B). As observed with the *ppk11^{DN}*, the *elav* × *ppk19^{DN}* cross also disrupted the preference for 10 mM NaCl (Figure 5D). In contrast, both the *elav* × *ppk4.15^{DN}* (Figure 5A) and the *elav* × *ppk28^{DN}* (Figure 5D) transgenic controls showed a salt-taste preference that was the same as wild-type. These data indicate that expressing dominant-negative PPK11 or PPK19 proteins impaired the ability of larvae to detect low concentrations of salt.

Disruption of the Behavioral Response to Salt with RNAi for PPK Constructs

Although dominant-negative PPK4 and PPK28 constructs produced no behavioral defect, we cannot exclude the possibility that PPK11^{DN} and PPK19^{DN} heteromultimerized with the other PPK subunits and disrupted their function. Therefore, to disrupt PPK function in a different way, we used the Gal4/UAS system to express double-stranded RNA (dsRNA) for RNA interference (RNAi) (Kalidas and Smith, 2002; Kennerdell and Carthew, 2000; Zamore et al., 2000). We examined the effect on *ppk11* mRNA levels using real-time, quantitative RT-PCR from third instar larvae. Because *ppk11* is expressed not only in neurons but also in the tracheal system, the fat body, and other cells, we tested two promoters to drive *ppk11^{dsRNA}* expression in these tissues: the *ppk11* promoter and the heat shock promoter. Table 2 shows that the *ppk11* × *ppk11$^{dsRNA.6}$* cross reduced *ppk11* transcripts slightly but not to a statistically significant extent, consistent with the conclusion that it is a relatively weak promoter. In contrast, the *HS* ×

Figure 1. Predicted Protein Sequence of the 16 Cloned Members of the PPK Family

Alignment of sequences was by Clustal W, with manual adjustments. The order of the different PPK genes was determined by the Clustal W program. The gray highlighted regions represent the first and second predicted transmembrane domains M1 and M2. The yellow highlighted and numbered residues indicate the conserved cysteine residues in the extracellular domain. The blue highlighted residues preceding M2 indicate the "Deg" residue, at which all the previously reported DEG/ENaC proteins contain a small side-chained residue of glycine, serine, or alanine. Conserved residues are highlighted in black, motifs that are highly conserved in DEG/ENaC family members are indicated in red, and potential N-linked glycosylation sites are in blue. Sequences that are spliced out in some transcripts are in green and underlined. A C-terminal sequence present in ENaC subunits is in pink. Construction of the *ppk14*, *ppk20*, and *ppk21* cDNAs is incomplete, and portions of their sequences were predicted based on the genomic sequence. PPK14 amino acid sequence was predicted after residue 387, PPK20 after residue 382, and PPK21 after residue 347. All sequence data are available from GenBank.

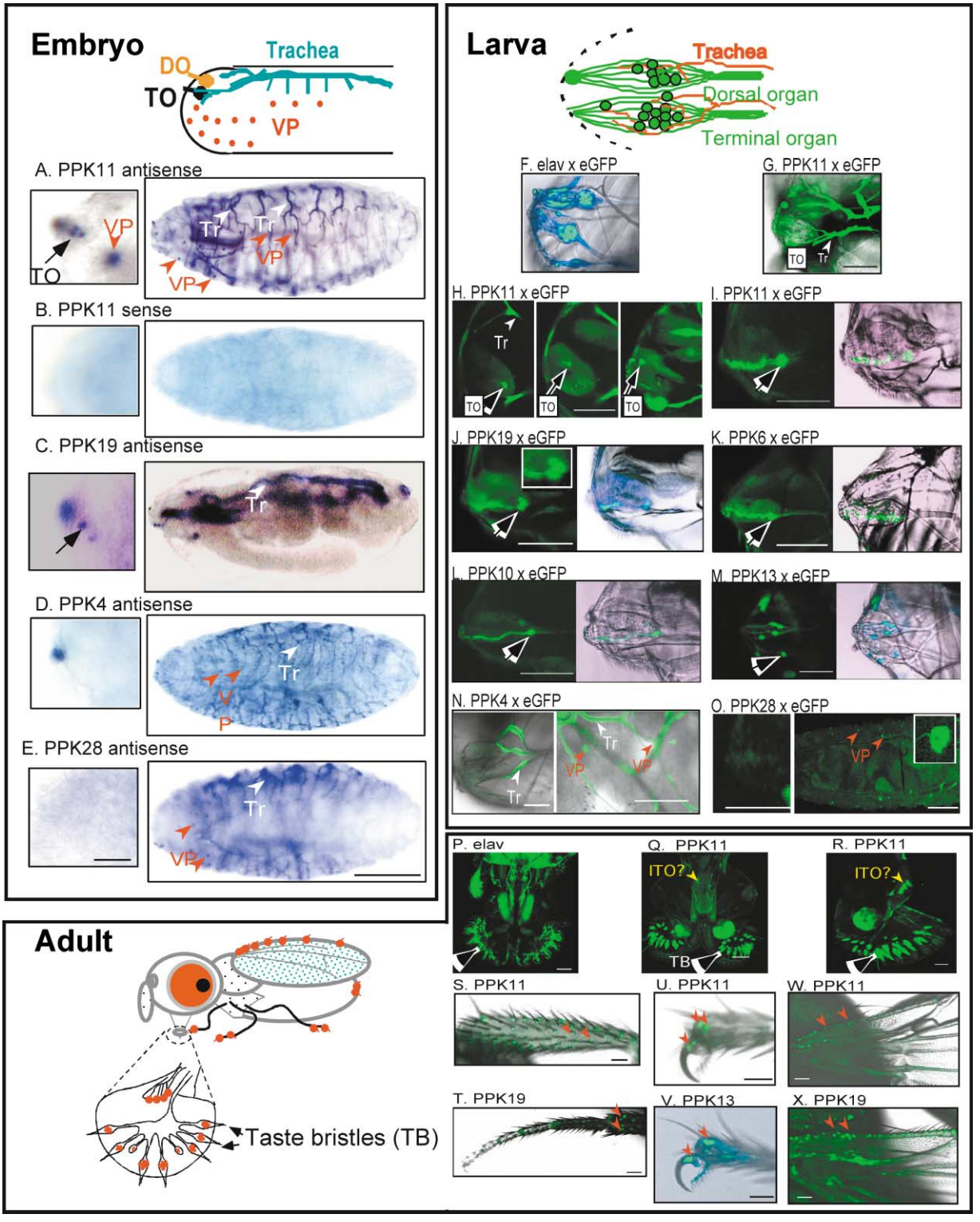

Figure 3. PPK Expression in Embryos, Larvae, and Adults

In all figures, anterior is to the left, dorsal is to the top of the page. For images (A)–(E), white arrowheads indicate the tracheal system (Tr); red arrowheads indicate ventral pits (VP). Scale bars are 100 μm in all images. (A–E) In situ hybridization of stage 16-17 embryos. Diagram at top shows tracheal system, terminal and dorsal organs, and ventral pits. (A) *ppk11* antisense probe shows staining in the tracheal system, ventral pits, and three cells in the terminal organ. Inset shows enlarged view of terminal organ (black arrow). The staining to the left of the three terminal organ neurons was variably observed and sometimes present with sense probe. It was also present in panels (C) and (D). Its identity and significance are not known. (B) *ppk11* sense probe shows no specific staining. (C) *ppk19* antisense probe showed staining in the terminal organ (black arrow). (D) Ventral view of *ppk4* antisense probe shows the tracheal system and ventral pits. (E)

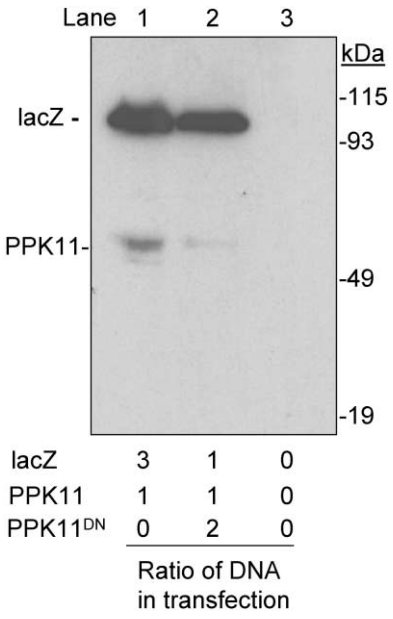

Figure 4. Effect of PPK11^{DN} Construct on PPK11 Production in *Drosophila* S_2 Cells

Numbers at bottom indicate ratio of cDNA. Total amount of cDNA was constant at 19 μg, and PPK11 cDNA was constant at 4.25 μg. Lane 1 shows PPK11 protein expression without dominant-negative PPK11 (PPK11^{DN}). Lane 2 shows PPK11 expression in the presence of PPK11^{DN} expression. Lane 3 shows the untransfected control.

ppk11$^{dsRNA.6}$ cross reduced *ppk11* transcripts by 7.7 ± 1.6-fold. These data indicate that RNAi can reduce *ppk11* mRNA.

We tested the ability of five independent *ppk11*^{dsRNA} lines to discriminate between water and 10 mM NaCl. Larvae from the *elav* × *ppk11*$^{dsRNA.6}$ cross showed defective salt-taste behavior (Figure 5C). The other four lines showed no defect, consistent with the reported low efficiency of heritable RNAi (Kalidas and Smith, 2002). When we used the heat shock promoter to express *ppk11*$^{dsRNA.6}$, salt taste was also defective (Figure 5C). The behavioral response to 10 mM NaCl was also disrupted in *elav* × *ppk19*^{dsRNA} transgenes (Figure 5D).

Selective Defects in Salt Taste in PPK11^{DN} Larvae

The attraction to 10 mM NaCl was not an osmotic effect, because larvae showed no preference for 20 mM manni-

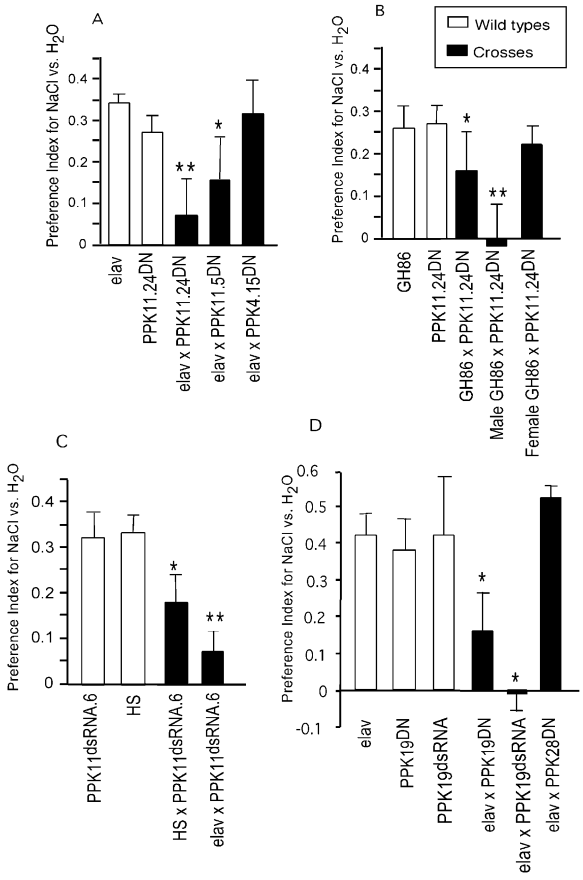

Figure 5. Salt-Taste Behavioral Assay

Preference index for 10 mM NaCl versus H_2O was calculated as $PI_{NaCl} = (N_{NaCl} - N_{H20})/(N_{NaCl} + N_{H20})$, where N is the number of larvae. Different genotypes are listed along x axis. The Gal4/UAS crosses were all heterozygous. (A) Effect of expressing a dominant-negative PPK11 construct with the elav panneuronal promoter on the preference index for a low salt concentration. (B) Effect of driving a PPK11^{DN} construct with the X chromosome GH86 promoter. (C) Effect of expressing a PPK11 double-stranded RNA. For the HS × PPK11$^{dsRNA.6}$ cross, 1 hr heat shock was given at 37°C each day for 4 days before the behavioral assay. (D) Effect of expressing PPK19^{DN} and PPK19^{dsRNA}. For each condition, 6 to 14 trials were performed with a total of 156 to 632 larvae tested for each condition. Black bars indicate crosses. *$p < 0.05$, **$p < 0.01$.

Ventral view of *ppk28* antisense probe shows the tracheal system and ventral pits. (F–O) Confocal images from promoter-driven eGFP in second instar larvae. Diagram at top shows terminal and dorsal organs (in green) and trachea (in red). In all images but (H) and (O), fluorescence image is overlaid on differential interference contrast image. (F) eGFP expression in neurons of the dorsal (DO) and terminal (TO) organs in an *elav* × *eGFP* cross. (G) *ppk11* × *eGFP* showing expression in the tracheal system and terminal organ. (H) Images are three confocal planes through the terminal organ showing three eGFP positive neurons (arrows). (I) Confocal images showing eGFP expression that extends out into the dendrites of two terminal organ neurons. (J) *ppk19* promoter expression in three neurons in terminal organ (arrow). (K) *ppk6* promoter expression in one terminal organ neuron (arrow). (L) *ppk10* promoter expression in one terminal (arrow) and one dorsal organ neuron. (M) PPK13 promoter expression in one terminal (arrow) and four dorsal organ neurons. (N) *ppk4* promoter-driven *UAS-eGFP* expression in the tracheal system and ventral pits. (O) *ppk28* promoter expression in ventral pits (right, arrow heads) and lack of expression in the terminal and dorsal organs (left). (P–X) Confocal images of eGFP expression in the adult. Diagram shows lateral view of adult, emphasizing the labelum of the probosis and some of the taste bristles (TB). (P) Confocal image from elav-driven eGFP showing labeling of all neurons in the proboscis. (Q and R) Confocal stacked image of *ppk11* promoter-driven eGFP expression in taste bristles in the labelum of proboscis (frontal view in [Q] and lateral view in [R]). The yellow arrowhead points to neurons that probably belong to the internal taste organ (ITO). (S) Expression of *ppk11* promoter in male tibial hair. (T) Expression of *ppk19* promoter in hairs of the prothoracic femur but not the tarsus. (U and V) Expression of the *ppk11* and *ppk13* promoters in the male tarsus. (W and X) Expression of the *ppk11* and *ppk19* promoters in the wing margin.

Table 2. Real-Time PCR

Drosophila Line	Number of Tests	Transcripts (Fold-Change)	P (t-test)
Wild-type	9	1.0	
ppk11 × *ppk11$^{dsRNA.6}$*	3	−2.8 ± 1.8	0.16
HS × *ppk11$^{dsRNA.6}$*	3	−7.7 ± 1.6	0.013
elav × *ppk11.24^{DN}*	3	+44.0 ± 14.3	0.037

The parental lines used as wild-type controls including *elav-Gal4*, *UAS-ppk11$^{dsRNA.6}$*, *HS-Gal4*, and *UAS-ppk11.24^{DN}*, each with two to three repetitions. The level of wild-type transcripts is defined as 1.0. Data are fold change in amount of transcripts; "−" indicates a decrease, and "+" indicates an increase. The *elav* × *ppk11.24^{DN}* cross served as a control. We did not test the *elav* × *ppk11$^{dsRNA.6}$* cross because the extensive *ppk11* expression in the tracheal system (Liu et al., 2003) would mask any effect of *ppk11$^{dsRNA..6}$* expression in the terminal organ neurons.

tol versus water (Figure 6A). One study suggested that the NaCl preference might result from Cl^- sensing (Miyakawa, 1982). However, Na^+ gluconate (10 mM) attracted wild-type but not *elav* × *ppk11.24^{DN}* larvae, suggesting that Cl^- was not required (Figure 6A). Consistent with this conclusion, wild-type larvae preferred 10 mM KCl to water and to 10 mM NaCl; these preferences were disrupted in *elav* × *ppk11.24^{DN}* larvae. We tested several other taste and olfactory chemicals and found that wild-type and *elav* × *ppk11^{DN}* larvae showed similar responses to acid (pH 3), butanol, and propionic acid. These results suggest that the defect in response to salt is not a generalized, nonspecific effect of the dominant-negative construct.

Effect of Disrupting PPK11 and PPK19 on the Response to High Salt Concentrations in Larvae

Low salt concentrations attract mammals, whereas high salt concentrations are repulsive (Denton, 1982). In electrophysiological studies, low salt concentrations stimulate narrow spectrum "salt-best" taste receptor cells, whereas high salt concentrations stimulate broad spectrum taste receptor cells that also respond to other agents, including bitter-tasting chemicals (Contreras and Lundy, 2000). Thus, it is likely that detection of high salt concentrations involves additional pathways. To determine the contribution of PPK11 to the detection of high salt concentrations, we examined the response to a range of NaCl concentrations (Figure 6B). Despite a disruption in the preference for 10 and 200 mM NaCl, larvae expressing the *ppk11^{DN}* construct rejected NaCl at concentrations of 500 and 1000 mM. *elav* × *ppk19^{DN}* showed a similar rejection of 500 mM NaCl (preference index, −0.41 ± 0.07, n = 101). These results suggest that additional mechanisms contribute to the detection of high salt concentrations. Consistent with this conclusion, we noted that when larvae crawled onto the surface of agarose containing high salt, they often twisted their bodies vigorously, a behavioral pattern similar to that associated with painful stimuli.

It has been reported that amiloride can inhibit the response to sweet stimuli in mammals and insects (Jenkins and Tompkins, 1990; Liscia and Solari, 2000; Mierson et al., 1988; Schiffman, 1983). We found that both *elav* × *ppk11^{DN}* and *elav* × *ppk19^{DN}* transgenics showed a normal behavioral preference for 500 mM sucrose versus water (Figure 6C). Adding 500 mM NaCl to the 500 mM sucrose elicited an aversive behavioral response in larvae as previously reported in adults (Dethier, 1976; Jenkins and Tompkins, 1990; Nakamura et al., 2002). Expressing *ppk19^{DN}* blunted this repulsive behavior, and *ppk11^{DN}* tended to decrease the aversive response although the data were not statistically significant (Figure 6C). These data suggest that in the larval terminal organ PPK subunits also make a contribution to the aversive response to high salt concentrations.

Response of Adult *Drosophila* to Sucrose and Salt

Expression of *ppk11* and *ppk19* in the adult labelum, tarsi, and wing margins suggested that disrupting their function could alter the response to salt. Previous work showed that adult *Drosophila* rejected salt concentrations of 500 mM (Balakrishnan and Rodrigues, 1991). To test this behavior, we used a modification of the chemical consumption assay (Ford and Tompkins, 1985). After an 18 hr period with free access to water but not food, we placed adults in a chamber and measured the percentage that consumed water during a 1.5–2 hr test period. Figure 6D shows that there was no difference between the tested genotypes. Including 300 mM NaCl in the water markedly reduced the percentage of wild-type and *elav* × *ppk28^{DN}* control animals that consumed liquid. However, disrupting PPK11 or PPK19 (*elav* × *ppk19^{RNA}*, *elav* × *ppk11^{RNA}* and *ppk11.24^{DN}*) reduced the percentage of animals that rejected the salt solution (Figure 6D). *elav* × *ppk19^{DN}* adults showed no defect in this assay (data not shown); perhaps the dominant-negative construct is less effective than the *ppk19^{dsRNA}* in these animals (for example, see Figure 5D in larvae). Thus, in both larvae and adults, PPK11 and PPK19 contribute to the behavioral response to salt.

Electrophysiologic Response to Low Salt

We used a previously reported method for extracellular recording of terminal organ nerve activity (Opplinger et al., 2000). To test the electrophysiologic response of the terminal organ, we placed a glass electrode over the terminal or dorsal organ, thereby both applying the salt solution and establishing the connection for extracellular recording. The dorsal organ showed no response to salt application (Figure 7A). The wild-type terminal organ responded to 10 mM KCl application with action potentials. In *elav* × *ppk11.24^{DN}* and *elav* × *ppk11$^{dsRNA.6}$* larvae, the spike frequencies were reduced by 30%–40% (Figure 7B); the differences were most prominent during the first 5 s after salt stimulation. In the behavioral assay, larvae discriminated between 10 mM KCl and 10 mM NaCl (Figure 6A). Electrophysiologic recordings also detected a difference between these salts; during the first second after a salt stimulus was applied to the terminal organ, 10 mM NaCl elicited 39 ± 2 spikes/s (n = 7) compared to 49 ± 2 spikes/s for 10 mM KCl (n = 9, $p < 0.01$).

Because amiloride can inhibit some DEG/ENaC channels (Garty and Palmer, 1997) and because a previous report indicated that 5 mM amiloride blunted the behavioral response to 100 mM NaCl in larvae (Jenkins and

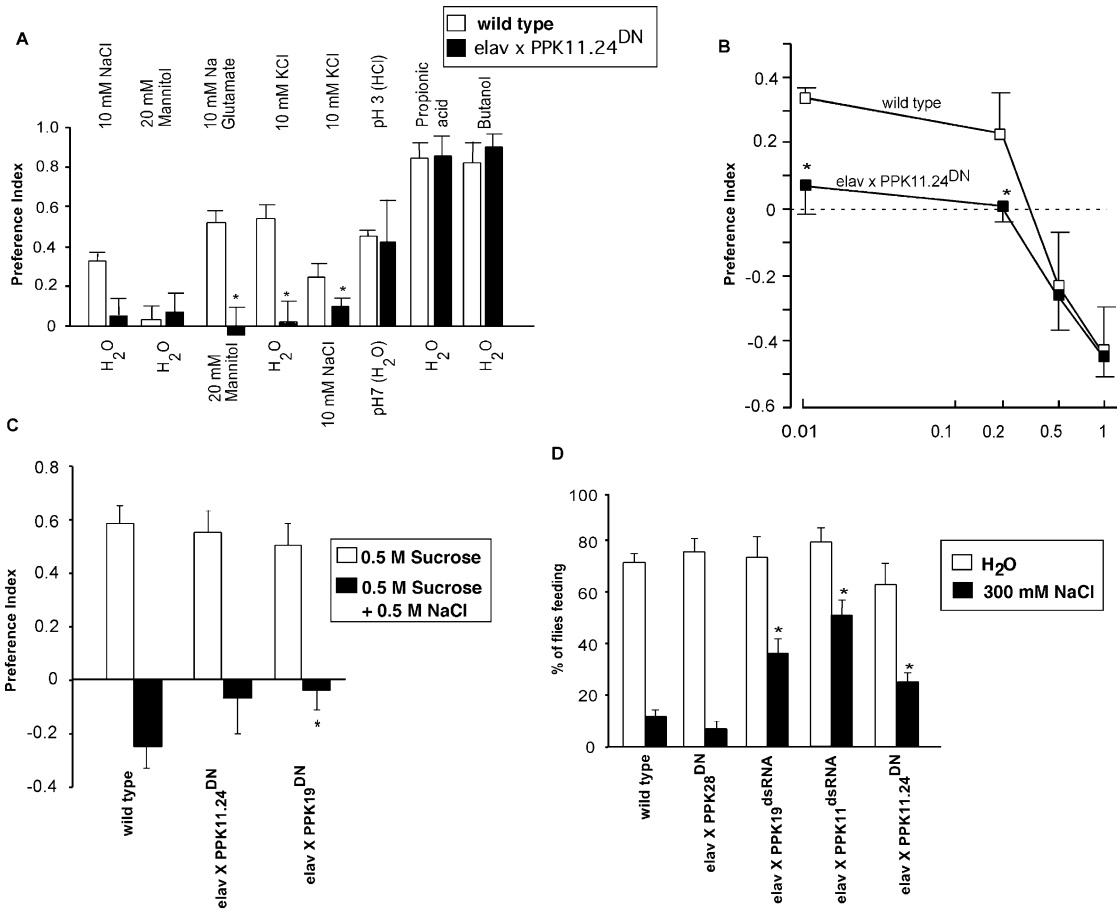

Figure 6. Behavioral Assay for Taste and Olfaction

(A) Preference for tastants and odors listed at top of graph versus those listed at bottom. Open bars indicate wild-type (*elav-Gal4* and *UAS-ppk11.24^{DN}*); filled black bars indicate a homozygous *elav* × *ppk11.24^{DN}* cross. Three to seven trials were done with each pair of tastants and odors, with a total of 97 to 213 larvae tested for each condition. (B) Effect of salt concentration on preference index. Data are preference for the indicated salt concentration versus water. Five to seven trials were performed, with a total of 102 to 153 larvae tested for each condition. *$p < 0.05$. (C) Preference to sucrose or sucrose plus salt. Ten trials were performed, with a total of 142 to 173 larvae tested for each condition. *$p < 0.01$. (D) Adult solution consumption assay. Six to eighteen trials were performed, with a total of 231 to 1469 adults tested for each condition. *$p < 0.001$.

Tompkins, 1990), we also examined its effect. Consistent with the previous report, we found that 5 mM amiloride attenuated the larval preference for 10 mM NaCl (Figure 8A). When we tested the electrophysiologic response, 5 mM but not 1 mM amiloride reduced the spike frequency response to 10 mM NaCl by about 40% (Figure 8B). These results are consistent with the ability of amiloride to inhibit some DEG/ENaC channels. However, the high concentration required may reflect limited sensitivity of PPK channels.

Discussion

Specific PPK11 Genes Are Expressed in Neurons that Detect Low Salt Concentrations

The larval terminal organ contains the receptors for salt taste (Heimbeck et al., 1999; Opplinger et al., 2000). Within the terminal organ, in situ hybridization and transgenic reporter expression revealed *ppk11* and *ppk19* each expressed in 3 of the approximately 30 neurons. We also detected larval terminal organ expression of *ppk6*, *ppk10*, and *ppk13* based on the pattern of reporter gene expression. In the adult, the *ppk11* promoter drove expression in the taste bristles of the labelum, which mediate the gustatory response to salt (Pollack and Balakrishnan, 1997; Singh, 1997). Moreover, *ppk11*, *ppk19*, and *ppk13* were expressed in peripheral locations previously implicated in adult gustation, including hairs on the legs, the tarsi, and the wing margins. Both the larval terminal organ and the adult labelum taste bristles consist of bipolar taste receptor neurons surrounded by supporting cells; this arrangement forms a specialized structure containing a pore at its tip (Singh, 1997). Thus, localization of PPK subunits in these specialized sensory neurons positions them where they could detect changes in salt concentration. Although our current data do not allow us to determine whether different PPK subunits are coexpressed in the same cells, expression of multiple PPK genes in the terminal organ raise the possibility that heteromultimeric channel complexes are formed.

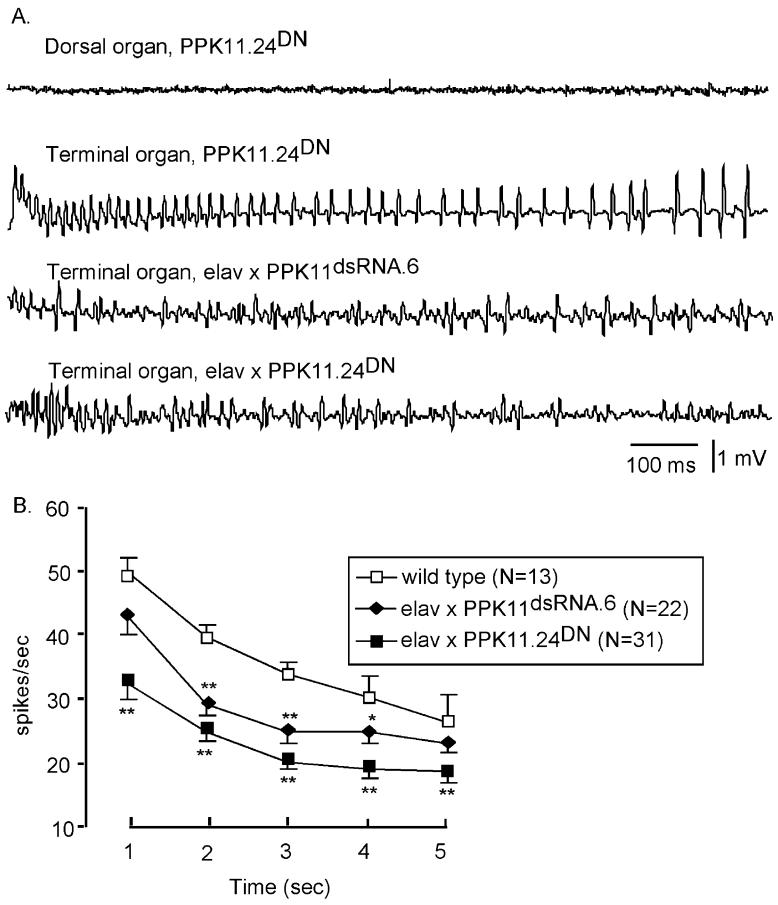

Figure 7. Electrophysiological Recordings from the Larval Terminal Organ

(A) Examples of electrophysiologic response to 10 mM KCl applied to the dorsal and terminal organs. Each trace is 1 s and begins with the initial contact of the terminal organ. (B) Electrophysiologic response to 10 mM KCl during first 5 s of recording. Data are spikes/s during sequential 1 s recording intervals. The heterozygous *elav* × *ppk11*$^{dsRNA.6}$ line and the homozygous *elav* × *ppk11.24*^{DN} line were used in this experiment. *p $<$ 0.05 versus wild-type, **p $<$ 0.01.

Disrupting PPK11 and PPK19 Function Impairs the Response to Low Salt Concentrations

Impairment of PPK11 and PPK19 function with dominant-negative constructs or RNAi disrupted the normal behavioral and electrophysiologic responses of larvae to low salt concentrations. In contrast, the normal response to acid and odorants suggested that some nonspecific effect or defective action potential generation was not responsible. Thus, the localization and the functional data suggest that PPK11 and PPK19 play an important role in detecting low salt concentrations.

The response to high salt concentrations was more complex. Earlier studies suggested that detection of low and high salt concentrations involve different receptor cells (Contreras and Lundy, 2000; Denton, 1982). We found that larvae with disrupted PPK11 or PPK19 function lost the preference for low salt concentrations but retained the aversive response to high salt concentrations. However, disrupting PPK19 function in larvae blunted the aversive effect of 500 mM NaCl when it was tested in the presence of sucrose. In adults, disrupting PPK11 or PPK19 reduced the aversive behavioral response to 300 mM NaCl. Thus, PPK11 and PPK19 may contribute to both the low and high salt concentration response, but other pathways are also probably involved in the aversive response to high salt concentrations. Additional evidence that the aversive response to high salt concentrations may be complex comes from reports that humans find high salt concentrations to have a bitter taste (Murphy et al., 1981; van der Klaauw and Smith, 1995).

PPK Subunits May Function as a Component of a Heteromultimeric Complex

DEG/ENaC subunits associate as homo- and heteromultimers to generate cation channels. For example, functional studies of DEG/ENaC knockout mice indicate that ASIC1, ASIC2, and ASIC3 subunits combine to generate H^+-gated currents in dorsal root ganglion neurons (Benson et al., 2002; Xie et al., 2002). In an attempt to generate currents, we expressed wild-type PPK11, PPK11 with a Deg mutation (G456V), and PPK11 together with several other PPK subunits (including some PPK subunits containing a Val at the Deg position) in *Xenopus* oocytes (data not shown). However, we observed no current. These results are consistent with results obtained with many other DEG/ENaC subunits. For example, heterologous expression of α, β, and γENaC generates constitutively active channels, whereas expression of β and/or γENaC produce no current, and expression of αENaC alone generates only very small currents (Canessa et al., 1994; McDonald et al., 1995). In addition, current generation by *C. elegans* DEG/ENaC subunits may require expression of multiple subunits plus associated cytosolic or extracellular proteins (Goodman et al., 2002; Tavernarakis and Driscoll, 1997).

Detection of Low Salt Concentrations by PPK Subunits

Earlier studies reported that amiloride treatment reduced the gustatory response to NaCl but not KCl in rodents (Brand et al., 1985; Gannon and Contreras, 1995; Heck et al., 1984). That finding, plus the observation that

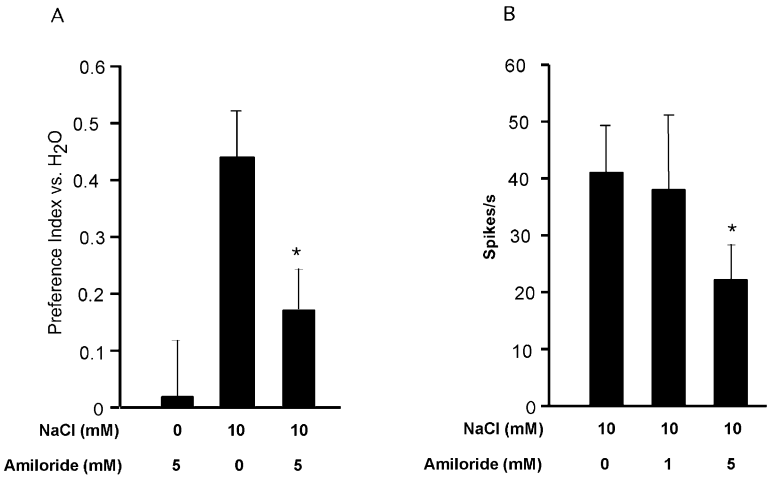

Figure 8. Amiloride Effect on the Response to Salt

(A) Behavioral preference to 10 mM NaCl in the presence and absence of amiloride. Eight trials were preformed, with a total 109 to 123 larvae. (B) Eletrophysiologic response to 10 mM NaCl with or without 5 mM amiloride. n = 10. *$p < 0.05$.

some DEG/ENaC channels exhibit a greater Na^+ than K^+ permeability, led to the hypothesis that DEG/ENaC subunits might be involved in detecting Na^+ salts but not non-Na^+ salts. However, interfering with PPK11 function disrupted the behavioral and electrophysiologic responses to Na^+ and K^+. In some cases DEG/ENaC channels show little discrimination between Na^+ and K^+, and the subunit composition of a channel can determine ion selectivity. For example, expression of ASIC3 alone produced a H^+-gated Na^+-selective sustained current, but coexpression of ASIC3 with ASIC2b (which generates no current on its own) produced a cation nonselective current (Lingueglia et al., 1997). In addition, ASIC1 and heteromultimeric H^+-gated currents may show some Ca^{2+} conductance (Kovalchuk Yu et al., 1990; Sutherland et al., 2001). Ion selectivity can also be altered by mutation of the "Deg" residue; insertion of a residue with a bulky side chain at the Deg position of ASIC2 (G430V) produced a constitutively active channel with little selectivity between Na^+ and K^+ (Waldmann et al., 1996). Thus, although we were not able to produce currents by heterologous expression of PPK11, results with other DEG/ENaC subunits indicate that it may contribute to cation channels.

We speculate that PPK11, PPK19, and additional PPK subunits may form constitutively active, nonselective cation channels in the bipolar taste receptor neurons. An increase in either the Na^+ or K^+ concentration in the external environment would depolarize the neuron, generating action potentials. For a nonselective cation channel, the degree of depolarization to an equal concentration of Na^+ versus K^+ would depend upon the extracellular concentration of these cations prior to addition of salt; these values are not known.

As we discussed above, previous studies have suggested that DEG/ENaC channels may be involved in salt taste in mammals. Our evidence that several PPK genes are involved in salt taste in *Drosophila* raises the possibility that the mechanisms for detecting salt may have been conserved from flies to mammals. Identification of PPK11 and PPK19 sets the stage for the discovery of additional DEG/ENaC subunits and associated proteins involved in salt taste and for understanding how salt is detected.

Experimental Procedures

Database Searching and Cloning

Database searches were performed using the BLAST network server (National Center for Biotechnology Information). Most of the known DEG/ENaC family proteins were used as templates to search for candidate DEG/ENaC genes. The most effective sequences for searching were the second transmembrane domain M2. After identifying candidates, the conserved pieces of predicted protein sequence were used to generate predicted full-length cDNA sequences. To qualify as good candidates, fly sequences were required to contain most of the multiple conserved sequences present in known DEG/ENaC proteins. Then intron-exon boundaries were predicted, and primers for RT-PCR were designed to avoid predicted introns. To clone the ATG sequence at the start of the coding sequence, we designed one primer to the most 5′ in-frame ATG that included the His-Gly (HG) sequence that lays N-terminal to M1. We found no intron between the start methionine and the HG sequence in any family member that we examined; to our knowledge this is also true for other DEG/ENaC genes. To clone the stop codon, we designed a primer downstream of the predicted stop codon. If we found the predicted stop codon in the sense frame of the sequenced RT-PCR product, then we considered the predicted stop codon to be correct.

Adult poly A+ mRNA (Clontech, Palo Alto, CA) was used for RT-PCR. Two to four pairs of primers were used in the RT-PCR to clone each PPK cDNA. We also found that embryo and larval mRNA was positive for *ppk11* and *ppk19* transcripts by RT-PCR but not by Northern analysis.

Sequence Line Up and Phylogenetic Tree Generation

The protein sequence alignment shown in Figure 1 was generated by CLUSTAL W (http://clustalw.genome.ad.jp), and slight adjustments were made manually. For generation of the tree shown in Figure 2, sequences were aligned using the ClustalW algorithm in the software package BioEdit (Hall, 1999). The default alignment matrix in BioEdit, Pam-Dayhoff matrix was used for the protein alignment. The alignment was saved in PHYLIP format, and PHYLIP was used to create the tree (Felsenstein, 1989). To construct the tree, we used the distance method; the parsimony method gave very similar results. For statistical analysis, the bootstrap method in PHYLIP was used. Each sequence was sampled 100 times to create 100 separate data sets. A tree was built from each data set, and then a consensus tree was made from all trees, and bootstrap values were assigned to the branches. The consensus tree was then generated using the program TreeView (Page, 1996).

Experimental Animals and In Situ Hybridization

Drosophila stocks were reared on standard cornmeal-agar-molasses medium at room temperature (21°C–25°C). yw^{67C23} strain was used for in situ hybridization. *D. melanogaster* embryos were collected and fixed following a previously described protocol (Lehmann

and Tautz, 1994). We used 7–24 hr old embryos. Embryo stages were determined by the structural pattern in the head and body (Campos-Ortega and Hartenstein, 1997) and by their tracheal development pattern as described (Bate and Martinez Arias, 1993). *ppk* cDNA sequences (0.7–1.2 kb) for all the newly cloned family members were used for in situ hybridization. Digoxigenin-labeled sense and antisense probes were synthesized using a Digoxigenin-labeling kit (Roche Molecular Biochemicals, Indianapolis, IN).

Generation of Transgenic Fly Lines

yw^{67C23} or w^{1118} strains were used for transgenic injections. P element-mediated transformation and subsequent fly crossings were performed following standard techniques (Rubin et al., 1985). Promoter-Gal4 transgenes were generated from a Gal4 PTGAL vector (a gift from D.F. Eberl). A *ppk11* promoter extending 2 kb 5′ of the translational start site was amplified by PCR from genomic DNA purified from yw^{67C23} adult flies. It is possible that 2 kb does not encompass the entire *ppk11* promoter. However, this method was used successfully to study G protein-coupled taste receptor genes in *Drosophila* (Scott et al., 2001). Scott et al. showed that eight of fifteen promoters varying from 0.6 to 9 kb were expressed in taste-sensing organs. The transgenic *ppk11* promoter lines were crossed with *UAS-eGFP*. Second and third instar larvae were mounted on glass slides and examined using confocal microscopy.

For some studies, we used the *elav-Gal4* line that drives expression in all neurons. For expression in the terminal organ we used the *GH86-Gal4* line (a gift of Dr. Gertrud Heimbeck). We refer to crosses between two lines that drive gene expression with the Gal4-UAS system by referring to the promoter and the expressed transgenes. For example, a cross between an *elav-Gal4* line and an *UAS-eGFP* line is referred to as *elav* × *eGFP*.

To generate dominant-negative constructs for PPK4, PPK11, PPK19, and PPK28, a cDNA sequence coding for the N-terminal 105, 204, 110, and 166 amino acids were cloned into the pUAST vector. To generate a heritable *ppk11* RNAi construct, 500 bp of antisense sequence followed by 500 bp sense sequence to the PPK11 N-terminal portion of the cDNA was constructed in the pUAST vector. The *ppk19* RNAi construct contained a 713 bp antisense sequence to the C-terminal region followed by 359 bp of the sense sequence to the same C-terminal region; this allowed a linker sequence between the sense and antisense sequences.

Real-Time PCR

mRNA from the various genotypes was collected from ten third instar larvae and treated with DNase (Invitrogen, Inc.) to reduce contamination from genomic DNA. The method for real-time PCR followed a standard protocol (Applied Biosystems, Roche). PCR primers and probe were designed to a region coding the N terminus of PPK11 and extending from nucleotide 63 to nucleotide 130 as follows: the primers were 5′-CCTGAGGCCCAAACAATCA and 5′-AAGAAGCCAAATGAAAGAGCCA, and the probe was targeted to 5′-TCAAATGCCAGCCACTTCGCGTTT.

Assay for a Dominant-Negative Effect

Because of the lack of a PPK11 antibody, we assessed the dominant-negative effect in S2 cells. cDNAs for full-length wild-type PPK11, N-terminal truncated PPK11 coding the first 204 amino acids ($PPK11^{DN}$), and lacZ were cloned into the pMT-His-V5 C vector (Invitrogen, Inc.). The translated proteins were all fused to His6 and V5 epitopes. These cDNAs were expressed in the *Drosophila* S_2 cell line (Invitrogen, Inc.). For transfections, the total amount of DNA was constant at 19 μg per 2×10^6 cells. The amount of full-length *ppk11* wild-type cDNA was also constant at 4.25 μg. The amount of $ppk11^{DN}$ and *lacZ* cDNA was varied.

Cells were induced by adding 50 μM $CuS0_4$ in the culture medium for 48 hr. Then, the cells were collected by washing with PBS and centrifuged at 1000 × *g* for 5 min. The cell pellet was lysed with a modified RIPA buffer containing 10 mM Tris-Cl (pH 7.4), 150 mM NaCl, 1 mM EGTA, 1 mM EDTA, 1% Triton X-100, 0.1% SDS, 0.2 mM PMSF, 1 μM leupeptin, and 0.1 μM aprotinin. The lysate was centrifuged at 110,000 × *g* for 30 min and was further purified on Ni^{2+} agarose resin and loaded on SDS-PAGE. Immunoblotting was performed with a monoclonal anti-V5 antibody (Invitrogen, Inc.) and an anti-mouse secondary antibody conjugated to HRP (Amersham, Pharmacia, UK). Detection was with enhanced chemilumenescence.

Behavioral Assay

For taste and olfactory behavioral assays, a two-way choice petri dish was set up as described (Heimbeck et al., 1999; Jenkins and Tompkins, 1990). In brief, third instar larvae picked from the medium were washed and immediately placed in the middle of a petri dish covered with 1% agarose. Studies were done at room temperature (21°C–25°C). In the taste-behavior assay, the various chemicals were mixed into the 1% agarose, and each half of the dish contained a different chemical. For example, one half might contain 10 mM NaCl and the other half 10 mM KCl. In the olfactory-behavior assay, small filter papers contained odorant solutions or water were placed at opposite ends of the petri dish on top of the agarose. The distribution of the larvae on each side was recorded at 30 min. The preference index (*PI*) to chemical "A" as compared to chemical "B" was calculated as $PI_A = (N_A - N_B)/(N_A + N_B)$, where N is the number of larvae (Jenkins and Tompkins, 1990; Miyakawa, 1981)

Adult Behavioral Assay

We used a modified chemical consumption assay (Ford and Tompkins, 1985). In brief, 30 to 100 2- to 4-day-old adults were placed in a vial for 18–20 hr in the absence of food but with water-saturated cotton. Flies were then moved to the bottom of a cell culture dish (60 mm × 15 mm). Drops of the test solutions containing green food dye (three drops per 10 ml) were placed on the cover of the dish. After 1.5–2 hr, we determined the percentage of animals that consumed the test solution by counting flies with a green abdomen. All data in the manuscript represents the mean ± SEM.

Electrophysiological Recording

We used an extracellular recording technique for third instar larvae as described previously with some modification (Opplinger et al., 2000). Larvae were tied to a metal rod with fibers dissected from unscented dental floss. The rod and tail of the larvae were placed in a 100 mM KCl solution, taking care to avoid contact of the larvae head with the solution. A silver chloride reference electrode was connected to the larval body through KCl solution. The recording electrode was a glass pipette filled with the test salt 10 mM KCl (we used KCl because it gave the best signal-to-noise ratio). This pipette served as both a stimulating and recording electrode. Voltages between reference and recording electrodes (Axopatch-1D, Axon Instruments) were filtered at 100–10,000 Hz and digitized. The sampling interval was 100 μs. Data were displayed using p-Clamp7.0 software. For action potentials to be counted, they were required to be clearly larger than the baseline noise level and biphasic. Examination of multiple traces showed that salt elicited at least two types of spikes. Although we consistently observed smaller amplitude spikes in *elav* × $ppk11.24^{DN}$ and *elav* × $ppk11^{dsRNA.6}$ crosses, only the frequency response was evaluated. In addition to the response to 10 mM KCl, it is possible that these extracellular multiunit recordings may include the output of motor neurons, thermosensitive neurons, water receptor cells, and sucrose and bitter taste receptor cells.

Acknowledgments

We thank Drs. Lori L. Wallrath and Daniel F. Eberl for many helpful discussions. We thank Yuhong Li and Jinghui Xie for excellent technical assistance. We thank Rob Thompson for construction of the phylogenetic tree. We thank Dr. Daniel F. Eberl for the Gal4 expression p-element vector. We thank Dr. Gertrud Heimbeck for *GH86-Gal4* line. We thank Dr. Kevin Knudtson and the University of Iowa DNA Core Facility (Diabetes and Endocrine Research Center; supported by NIH # DK25295) for assistance with sequencing, oligonucleotide synthesis, and real-time PCR experiment. This work was supported by the HHMI and the National Institutes of Health (HL-14388 and HL-29851). M.J.W. is an Investigator of the HHMI.

Received: September 12, 2002
Revised: March 19, 2003
Accepted: May 27, 2003
Published: July 2, 2003

References

Adams, C.M., Snyder, P.M., and Welsh, M.J. (1997). Interactions between subunits of the human epithelial sodium channel. J. Biol. Chem. *272*, 27295–27300.

Adams, C.M., Anderson, M.G., Motto, D.G., Price, M.P., Johnson, W.A., and Welsh, M.J. (1998a). Ripped pocket and pickpocket, novel *Drosophila* DEG/ENaC subunits expressed in early development and in mechanosensory neurons. J. Cell Biol. *140*, 143–152.

Adams, C.M., Snyder, P.M., Price, M.P., and Welsh, M.J. (1998b). Protons activate brain Na^+ channel 1 by inducing a conformational change that exposes a residue associated with neurodegeneration. J. Biol. Chem. *273*, 30204–30207.

Balakrishnan, R., and Rodrigues, V. (1991). The shaker and shaking-B genes specify elements in the processing of gustatory information in Drosophila melanogaster. J. Exp. Biol. *157*, 161–181.

Bate, M., and Martinez Arias, A. (1993). The Development of *Drosophila melanogaster* (Cold Spring Harbor, NY: Cold Spring Harbor Laboratory Press).

Benson, C.J., Xie, J., Wemmie, J.A., Price, M.P., Henss, J.M., Welsh, M.J., and Snyder, P.M. (2002). Heteromultimerics of DEG/ENaC subunits form H^+-gated channels in mouse sensory neurons. Proc. Natl. Acad. Sci. USA *99*, 2338–2343.

Boughter, J.D., Jr., and Smith, D.V. (1998). Amiloride blocks acid responses in NaCl-best gustatory neurons of the hamster solitary nucleus. J. Neurophysiol. *80*, 1362–1372.

Brand, J.G., Teeter, J.H., and Silver, W.L. (1985). Inhibition by amiloride of chorda tympani responses evoked by monovalent salts. Brain Res. *334*, 207–214.

Campos-Ortega, J.A., and Hartenstein, V. (1997). The Embryonic Development of Drosophila Melanogaster, Second Edition (Berlin: Springer-Verlag).

Canessa, C.M., Schild, L., Buell, G., Thorens, B., Gautschi, I., Horisberger, J.D., and Rossier, B.C. (1994). Amiloride-sensitive epithelial Na^+ channel is made of three homologous subunits. Nature *367*, 463–467.

Chalfie, M., and Wolinsky, E. (1990). The identification and suppression of inherited neurodegeneration in Caenorhabditis elegans. Nature *345*, 410–416.

Contreras, R.J., and Lundy, R.F. (2000). Gustatory neuron types in the periphery: a functional perspective. Physiol. Behav. *69*, 41–52.

Darboux, I., Lingueglia, E., Pauron, D., Barbry, P., and Lazdunski, M. (1998). A new member of the amiloride-sensitive sodium channel family in *Drosophila melanogaster* peripheral nervous system. Biochem. Biophys. Res. Commun. *246*, 210–216.

Denton, D. (1982). The Hunger for Salt. An Anthropological, Physiological and Medical Analysis (Berlin: Springer-Verlag).

DeSimone, J.A., Heck, G.L., and DeSimone, S.K. (1981). Active ion transport in dog tongue: a possible role in taste. Science *214*, 1039–1041.

Dethier, V.G. (1976). The Hungry Fly (Cambridge, MA: Harvard University Press).

Driscoll, M., and Chalfie, M. (1991). The *mec*-4 gene is a member of a family of *Caenorhabditis elegans* genes that can mutate to induce neuronal degeneration. Nature *349*, 588–593.

Felsenstein, J. (1989). PHYLIP Phylogengy inference package. Cladistics *5*, 164–166.

Ford, S., and Tompkins, L. (1985). An assay to measure the consumption of attractants in solution. Drosophila Information Service *61*, 72.

Frings, S., Lynch, J.W., and Lindemann, B. (1992). Properties of cyclic nucleotide-gated channels mediating olfactory transduction. Activation, selectivity, and blockage. J. Gen. Physiol. *100*, 45–67.

Gannon, K.S., and Contreras, R.J. (1995). Sodium intake linked to amiloride-sensitive gustatory transduction in C57BL/6J and 129/J mice. Physiol. Behav. *57*, 231–239.

Garty, H., and Palmer, L.G. (1997). Epithelial sodium channels: function, structure, and regulation. Physiol. Rev. *77*, 359–396.

Goodman, M.B., Ernstrom, G.G., Chelur, D.S., O'Hagan, R., Yao, C.A., and Chalfie, M. (2002). MEC-2 regulates C. elegans DEG/ENaC channels needed for mechanosensation. Nature *415*, 1039–1042.

Hall, T.A. (1999). BioEdit: a user-friendly biological sequence alignment editor and analysis program for Windows 95/98/NT. Nucl. Acids Symp. Ser. *41*, 95–98.

Halpern, B.P. (1998). Amiloride and vertebrate gustatory responses to NaCl. Neurosci. Biobehav. Rev. *23*, 5–47.

Heck, G.L., Mierson, S., and DeSimone, J.A. (1984). Salt taste transduction occurs through an amiloride-sensitive sodium transport pathway. Science *223*, 403–405.

Heimbeck, G., Bugnon, V., Gendre, N., Haberlin, C., and Stocker, R.F. (1999). Smell and taste perception in Drosophila melanogaster larva: toxin expression studies in chemosensory neurons. J. Neurosci. *19*, 6599–6609.

Herness, M.S., and Gilbertson, T.A. (1999). Cellular mechanisms of taste transduction. Annu. Rev. Physiol. *61*, 873–900.

Hong, K., Mano, I., and Driscoll, M. (2000). In vivo structure-function analyses of Caenorhabditis elegans MEC-4, a candidate mechanosensory ion channel subunit. J. Neurosci. *20*, 2575–2588.

Jenkins, J.B., and Tompkins, L. (1990). Effects of amiloride on taste responses of *Drosophila melanogaster* adults and larvae. J. Insect Physiol. *36*, 613–618.

Kalidas, S., and Smith, D.P. (2002). Novel genomic cDNA hybrids produce effective RNA interference in adult *Drosophila*. Neuron *33*, 177–184.

Kellenberger, S., Hoffman-Pochon, N., Gautschi, I., Schneeberger, E., and Schild, L. (1999). On the molecular basis of ion permeation in the epithelial Na^+ channel. J. Gen. Physiol. *114*, 13–30.

Kennerdell, J.R., and Carthew, R.W. (2000). Heritable gene silencing in Drosophila using double-stranded RNA. Nat. Biotechnol. *18*, 896–898.

Kinnamon, S.C., and Cummings, T.A. (1992). Chemosensory transduction mechanisms in taste. Annu. Rev. Physiol. *54*, 715–731.

Kinnamon, S.C., and Margolskee, R.F. (1996). Mechanisms of taste transduction. Curr. Opin. Neurobiol. *6*, 506–513.

Kovalchuk Yu, N., Krishtal, O.A., and Nowycky, M.C. (1990). The proton-activated inward current of rat sensory neurons includes a calcium component. Neurosci. Lett. *115*, 237–242.

Kretz, O., Barbry, P., Bock, R., and Lindemann, B. (1999). Differential expression of RNA and protein of the three pore-forming subunits of the amiloride-sensitive epithelial sodium channel in taste buds of the rat. J. Histochem. Cytochem. *47*, 51–64.

Lehmann, R., and Tautz, D. (1994). In situ hybridization to RNA. Methods Cell Biol. *44*, 575–598.

Lin, W., Finger, T.E., Rossier, B.C., and Kinnamon, S.C. (1999). Epithelial Na^+ channel subunits in rat taste cells: localization and regulation by aldosterone. J. Comp. Neurol. *405*, 406–420.

Lindemann, B. (1996). Taste reception. Physiol. Rev. *76*, 719–766.

Lingueglia, E., de Weille, J.R., Bassilana, F., Heurteaux, C., Sakai, H., Waldmann, R., and Lazdunski, M. (1997). A modulatory subunit of acid sensing ion channels in brain and dorsal root ganglion cells. J. Biol. Chem. *272*, 29778–29783.

Liscia, A., and Solari, P. (2000). Bitter taste recognition in the blowfly: Electrophysiological and behavioral evidence. Physiol. Behav. *70*, 61–65.

Littleton, J.T., and Ganetzky, B. (2000). Ion channels and synaptic organization: analysis of the *Drosophila* genome. Neuron *26*, 35–43.

Liu, L., Johnson, W.A., and Welsh, M.J. (2003). *Drosophila* DEG/ENaC pocket genes are expressed in the tracheal system may be involed in liquid clearance. Proc. Natl. Acad. Sci. USA *100*, 2128–2133.

Luciani, S., Bova, S., Cargnelli, G., and Debetto, P. (1992). Effects of amiloride on the cardiovascular system: role of Na^+/Ca2$^+$ exchange. Pharmacol. Res. *25*, 303–310.

Lundy, R.F., Jr., Pittman, D.W., and Contreras, R.J. (1997). Role for epithelial Na^+ channels and putative Na^+/H^+ exchangers in salt taste transduction in rats. Am. J. Physiol. *273*, R1923–R1931.

McDonald, F.J., Price, M.P., Snyder, P.M., and Welsh, M.J. (1995). Cloning and expression of the β- and γ-subunits of the human epithelial sodium channel. Am. J. Physiol. *268*, C1157–C1163.

Mierson, S., DeSimone, S.K., Heck, G.L., and DeSimone, J.A. (1988). Sugar-activated ion transport in canine lingual epithelium. Implications for sugar taste transduction. J. Gen. Physiol. *92*, 87–111.

Miyakawa, Y. (1981). Bimodal response in a chemotactic behaviour of *Drosophila* larvae to monovalent salts. J. Insect Physiol. *27*, 387–392.

Miyakawa, Y. (1982). Behavioural evidence for the existence of sugar, salt and amino acid taste receptor cells and some of their properties in *Drosophila* larvae. J. Insect Physiol. *28*, 405–410.

Murphy, C., Cardello, A.V., and Brand, J. (1981). Tastes of fifteen halide salts following water and NaCl: anion and cation effects. Physiol. Behav. *26*, 1083–1095.

Nakamura, M., Baldwin, D., Hannaford, S., Palka, J., and Montell, C. (2002). Defective proboscis extension response (DPR), a member of the Ig superfamily required for the gustatory response to salt. J. Neurosci. *22*, 3463–3472.

Opplinger, F.Y., Guerin, P.M., and Vlimant, M. (2000). Neurophysiological and behavioural evidence for an olfactory function for the dorsal organ and a gustatory one for the terminal organ in *Drosophila melanogaster* larvae. J. Insect Physiol. *46*, 135–144.

Page, R.D.M. (1996). TREEVIEW: An application to display phylogenetic trees on personal computers. Comput. Appl. Biosci. *12*, 357–358.

Pollack, G.S., and Balakrishnan, R. (1997). Taste sensilla of flies: function, central neuronal projections, and development. Microsc. Res. Tech. *39*, 532–546.

Python, F., and Stocker, R.F. (2002). Adult-like complexity of the larval antennal lobe of *D. melanogaster* despite markedly low numbers of odorant receptor neurons. J. Comp. Neurol. *445*, 374–387.

Rubin, G.M., Hazelrigg, T., Karess, R.E., Laski, F.A., Laverty, T., Levis, R., Rio, D.C., Spencer, F.A., and Zuker, C.S. (1985). Germ line specificity of P-element transposition and some novel patterns of expression of transduced copies of the white gene. Cold Spring Harb. Symp. Quant. Biol. *50*, 329–335.

Schiffman. (1983). Amiloride reduces the taste intensity of Na^+ and Li^+ salts and sweetners. Proc. Natl. Acad. Sci. USA *80*, 6136–6140.

Schild, L., Lu, Y., Gautschi, I., Schneeberger, E., Lifton, R.P., and Rossier, B.C. (1996). Identification of a PY motif in the epithelial Na channel subunits as a target sequence for mutations causing channel activation found in Liddle syndrome. EMBO J. *15*, 2381–2387.

Scott, T.R., and Giza, B.K. (1990). Coding channels in the taste system of the rat. Science *249*, 1585–1587.

Scott, K., Brady, R., Jr., Cravchik, A., Morozov, P., Rzhetsky, A., Zuker, C., and Axel, R. (2001). A chemosensory gene family encoding candidate gustatory and olfactory receptors in *Drosophila*. Cell *104*, 661–673.

Shanbhag, S.R., Park, S.K., Pikielny, C.W., and Steinbrecht, R.A. (2001). Gustatory organs of Drosophila melanogaster: fine structure and expression of the putative odorant-binding protein PBPRP2. Cell Tissue Res. *304*, 423–437.

Singh, R.N. (1997). Neurobiology of the gustatory systems of Drosophila and some terrestrial insects. Microsc. Res. Tech. *39*, 547–563.

Smith, D.P. (2001). *Drosophila* gustation: a question of taste. Neuron *29*, 551–554.

Snyder, P.M., Price, M.P., McDonald, F.J., Adams, C.M., Volk, K.A., Zeiher, B.G., Stokes, J.B., and Welsh, M.J. (1995). Mechanism by which Liddle's syndrome mutations increase activity of a human epithelial Na^+ channel. Cell *83*, 969–978.

Stocker, R.F. (1994). The organization of the chemosensory system in Drosophila melanogaster: a review. Cell Tissue Res. *275*, 3–26.

Sutherland, S.P., Benson, C.J., Adelman, J.P., and McCleskey, E.W. (2001). Acid-sensing ion channel 3 matches the acid-gated current in cardiac ischemia-sensing neurons. Proc. Natl. Acad. Sci. USA *98*, 711–716.

Tang, C.M., Presser, F., and Morad, M. (1988). Amiloride selectively blocks the low threshold (T) calcium channel. Science *240*, 213–215.

Tavernarakis, N., and Driscoll, M. (1997). Molecular modeling of mechanotransduction in the nematode *Caenorhabditis elegans*. Annu. Rev. Physiol. *59*, 659–689.

van der Klaauw, N.J., and Smith, D.V. (1995). Taste quality profiles for fifteen organic and inorganic salts. Physiol. Behav. *58*, 295–306.

Waldmann, R., Champigny, G., Voilley, N., Lauritzen, I., and Lazdunski, M. (1996). The mammalian degenerin MDEG, an amiloride-sensitive cation channel activated by mutations causing neurodegeneration in *Caenorhabditis elegans*. J. Biol. Chem. *271*, 10433–10436.

Waldmann, R., Champigny, G., Bassilana, F., Heurteaux, C., and Lazdunski, M. (1997). A proton-gated cation channel involved in acid-sensing. Nature *386*, 173–177.

Xie, J., Price, M.P., Berger, A.L., and Welsh, M.J. (2002). DRASIC Contributes to pH-gated currents in large dorsal root ganglion sensory neurons by forming heteromultimeric channels. J. Neurophysiol. *87*, 2835–2843.

Zamore, P.D., Tuschl, T., Sharp, P.A., and Bartel, D.P. (2000). RNAi: double-stranded RNA directs the ATP-dependent cleavage of mRNA at 21 to 23 nucleotide intervals. Cell *101*, 25–33.